



MULTIPLE MIRROR TELESCOPE OBSERVATORY

Smithsonian Astrophysical Observatory and Steward Observatory, University of Arizona

Reply to: MMT Observatory
University of Arizona
Tucson, Arizona 85721
(602) 621-1558

MMTO Internal Technical Memorandum 85-1

Subject: Autoguiding with the New Top Box

From: C. Janes and J. Montgomery

Date: June 27, 1985

Summary: Automatic guiding, that is closed loop control of the secondaries, was tested during M&E time June 14. The data show a factor of three improvement in tracking error between auto-guiding and open loop corrections, though the closed-loop errors are expected to be much better with a better selection of coefficients for the terms in the tracking algorithm.

Test setup: The experiment was conducted using the following equipment (refer to figure 1):

1. The new top box with the prism wheel at the pupil plane, the Fairchild intensified CCD TV camera as the acquisition camera, the 200 mm lens, and the AWP's at the home position (no offsetting).
2. A beam splitter on the "feed select" stage in the top box to deflect half of the telescope beam to a Pulnix unintensified CCD TV camera located in the lower level of the top box.
3. The MMT spectrograph 2 x 3 aperture plate at the focal plane.
4. The TCS computer and Grinnell image processor performing the usual auto-guiding operations.
5. The spare computer controlling the prism wheels in the top box proportional to parallactic angle.
6. The instrument computer and Grinnell image processor measuring star positions from video supplied by the Pulnix camera, using software transported from the TCS routine.

Test procedure: A 2.1 magnitude star was selected from the MMTO star catalogue with an azimuth of 235° and an elevation of 60° , and velocities of 20 and 10 arcseconds per second, respectively. The TCS routine was used to place the images in the "stacker" format, that is, in a line in elevation. Software limits were set for the instrument rotator of +5 PA and -20 PA to prevent damage to the spectrograph umbilical, and SKY-PA changed on the mount routine to bring ROT-PA within the MIN and MAX PA limits. The scale of the Pulnix was found to be 21.6 pixels per arcsecond as measured at the instrument computer. The auto-guiding update rate was set at 1 Hz. The FWHM of the individual images and the stacked images were taken before and after each test.

The prism wheel was inspected using close-up optics and the acquisition TV to insure that the individual telescope pupils were lined up with their respective wedges. To further insure that the pupils were aligned the 200 mm lens was selected, then each secondary was "nodded" and the video inspected to insure that the motion of one secondary did not introduce motion in more than one image at the acquisition camera.

The star was tracked using closed-loop corrections for 1024 seconds, and then the procedure repeated with open-loop corrections only. The closed loop corrections were applied to the secondaries by using a centroiding algorithm (classical) in the TCS computer to accurately locate each star image position on the acquisition TV video. In the the open loop test, an empirically determined flexure file was used to make secondary corrections. Mount tracking errors were corrected using an error look-up table in the mount computer for both tests.

The six image positions were measured every 2 seconds at the beam splitter using the Sony CCD and the instrument Grinnell and computer. The software used was ported from the TCS computer and first tested this night.

The top box derotator was used during both tests; the typical rotational velocity during the tests was approximately $-.20^{\circ}$ per minute.

Test results: The alignment of the pupils with the prisms, a configuration required for autoguiding, went very smoothly. A description of the alignment procedure and findings is in a separate Technical Memorandum.

Installing the prism wheel at the pupil plane normally causes the 6 telescope images to form a hexagonal pattern at the acquisition TV if the images are coincident at the focal plane. In this test, the images were lined up in a row at the focal plane as they would be for observing with the spectrograph stacker. The result was elongation of the hexagon in the vertical (elevation) direction, though there was no apparent change in the placement of the pupils on the prism wheel. Having the images in a row, permitted measurement of individual image position at the instrument computer. The results are shown in figures 2 through 7.

Peak-to-peak tracking error while making closed-loop corrections was measured to be .5 arcseconds in both axes (figures 2 and 4). A scale enlargement of this data (figures 6 and 7) shows good correlation of the error between the different secondaries. This seems to imply mount tracking error, but we are inclined to believe the correlated errors are more a result of bad coefficients selected for the terms in the tracking algorithm than lack of response to tracking error. We think the algorithm is over-correcting and introducing the error shown in the data. The correlated error in the open-loop tracking, however, is most likely caused by mount tracking errors. Although the peak-to-peak error of the closed-loop tracking is less than open-loop errors, a comparison at this point would be premature since adjusting correction coefficients in the tracking algorithm and changing the update rate are expected to improve the closed-loop tracking characteristics. More testing is needed to determine how to maximize the tracking parameters.

The drift in image position (most pronounced in image B, both in elevation and azimuth) is cause for concern. Closed-loop tracking data taken at the acquisition TV (Tech Memo 83-1) show no drift. The data are shown in the same order that the images appeared on the Sony target; it appears that the slope of the drift is a function of the image order. Apparent motion of the images at the acquisition camera introduced from whatever cause -- rotational axes not coaxial, Varo tube distortion, etc. -- will result in corrections to the secondaries that will cause real motion at the focal plane (Sony). Additional tests are necessary to find and correct the source of this measurement error. (Note added in proof: the derotator may not have been moving during these tests. If so, such an effect might occur. JM)

The FWHM measurements at the beginning and end of the closed-loop test were as follows:

	<u>el</u>	<u>az</u>	
Point stack at start	1.5	1.4	arcseconds
Finish before point stack	1.8	1.6	
Point stack at finish	1.8	1.6	

The same star was tracked for the next test, but with only open-loop flexure corrections applied. The tracking error was measured to be 1.5 arcseconds peak-to-peak (figures 3 and 5). Again the bulk of this error is correlated between telescopes indicating mount tracking error, but at a magnitude three times that measured while auto-guiding. Notice that image drift is still present, but the relative slopes of the drifts are different from those seen with auto-guiding, and an order dependent on image position is not evident.

The FWHM measurements at the beginning and end of the open-loop test were as follows:

	<u>el</u>	<u>az</u>	
Point stack at start	1.7	1.4	arcseconds
Finish	1.8	1.5	

Conclusions:

The test showed that closed-loop operation now can be dependably setup in a reasonable length of time. The alignment problems have been corrected, and the equipment and software is in place to test the procedure. The following questions remain:

1. What causes the images to drift on the Sony during closed-loop operation? Does the pattern change with image order, camera rotation, relative location of rotational axes, sky position?
2. What component of correlated error in closed-loop is tracking error, what seeing, and what caused by poorly tuned coefficients?
3. How are closed-loop coefficients optimized for different sampling rates?

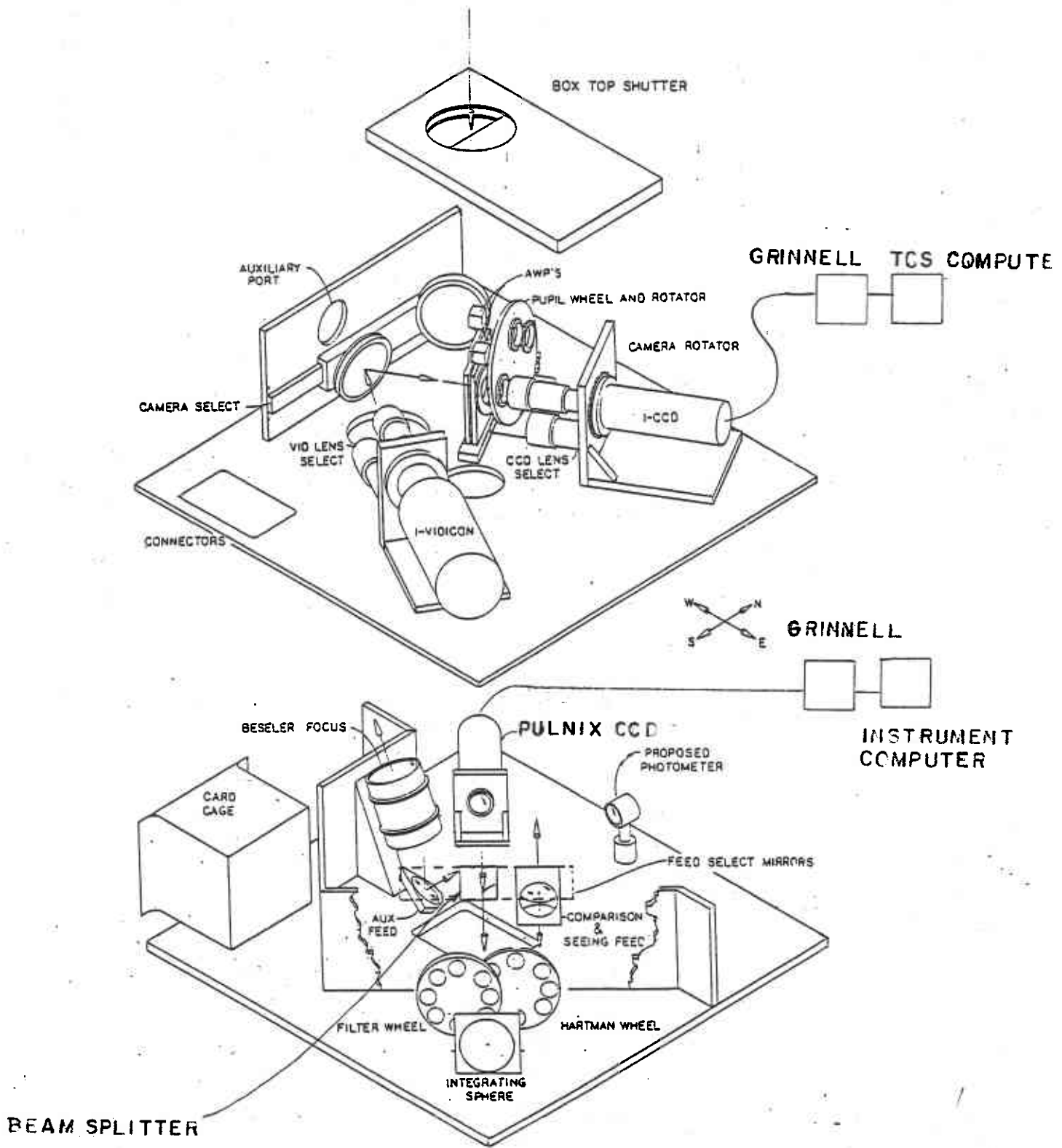


FIGURE 1
TOP BOX LAYOUT FOR AUTOGUIDING TEST

IMAGE B

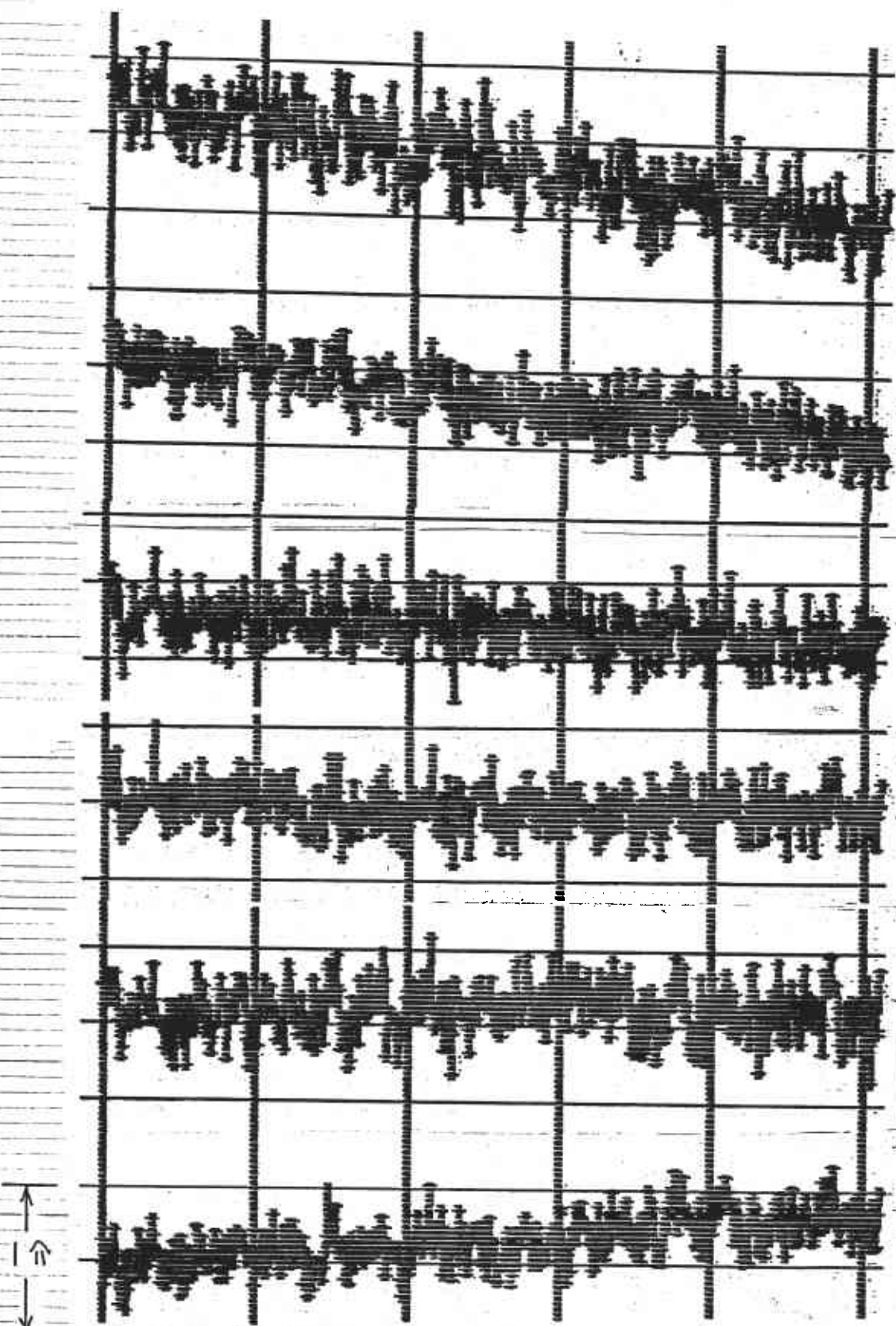
IMAGE C

IMAGE A

IMAGE F

IMAGE D

IMAGE E



0 200 400 600 800 1000 SECONDS

IMAGE MOTION IN ELEVATION WHILE
AUTOGUIDING, 6-14-85

FIGURE 2

FIGURE 3

IMAGE MOTION IN ELEVATION, OPEN LOOP,

6-14-85

